Int. J. Radiation Oncology Biol. Phys., Vol. 37, No. 2, pp. 455–463, 1997

0360-3016/97 $17.00 + .00

ELSEVIER

PII S0360-3016(96)00496-8

● *Physics Contribution*

THREE-DIMENSIONAL APPLICATOR SYSTEM FOR CARCINOMA OF THE UTERINE CERVIX

K. J. WEEKS, PH.D. AND G. S. MONTANA, M.D.

Department of Radiation Oncology, Duke University Medical Center, Durham, NC

Purpose: Intracavitary dose prescription for cancer of the uterine cervix has been based on the use of plane orthogonal films. Computed tomography (CT) and magnetic resonance imaging can provide three-dimensional (3D) anatomic information with which more sophisticated treatment planning can be carried out. This work describes a new tandem and ovoids design that permits modern 3D dosimetry and has the same placement flexibility for the physician as the applicators currently being used.

Methods and Materials: The external shape of the Fletcher–Suit–Delclos (FSD) minicolpostat tandem and ovoids system has been used as a model to build a prototype of a new applicator. The prototype colpostats are constructed out of aluminum and steel. The tandems are made of aluminum. The Fletcher shields are eliminated. A new method of using tungsten for dose attenuation and shielding has been designed. Longitudinal alignment of the tungsten shields makes the new system possible. This applicator is CT-compatible.

Results: Dose calculations for the new design are compared to a commercial version of the FSD applicator. Both the aluminum prototype and a simple extension of the prototype to a plastic applicator system are considered. It is shown that the principal difference in dose is that the dose is reduced in the region inferior to the center of the ovoids. All configurations (plastic caps on or off) are equivalently shielded for the new device. In addition, an intermediate mini-ovoid configuration can be used clinically via the introduction of a *D*-shaped cap. The latter reduces the high dose to the vaginal mucosal surfaces.

Conclusion: For a single ovoid, a comparison of dose with the FSD shows differences; however, the difference in dose is insignificant when the complete applicator, tandem, and ovoids are compared. With this new applicator, it is now possible to accumulate very accurate and detailed 3D dose-distribution data for the critical structures and other points of interest in the vicinity of the applicator. These data will permit future analysis of the correlation of dose and outcome for carcinoma of the cervix. © 1997 Elsevier Science Inc.

Fletcher–Suit–Delclos, CT, Tandem and ovoids, Cervix cancer, Brachytherapy, Applicators.

INTRODUCTION

The Fletcher (4) intracavitary applicator for the treatment of cancer of the uterine cervix was developed on the basis of the experience of the Manchester tandem and ovoid system (22), designed for use with radium sources. The original preloaded system was modified by Suit *et al.* (21) and converted to an afterloading system to reduce exposure to personnel. Other improvements (1, 3, 5, 7) followed and culminated in Delclos's design of minicolpostats for use when the vaginal vault is narrow or distorted (8). An important aspect of the Fletcher applicator design is the use of high-density metal shields to reduce the dose in the direction of the anterior rectal wall and the bladder trigone without decreasing the dose to the cervix and paracervical areas (2, 4).

With the Fletcher system, to obtain the most desirable dose distribution, the ovoids should be close to the vaginal apex and separated from each other as much as possible. The metal shields in the ovoids (typically tungsten alloy) of the system provide additional sparing of the bladder and rectum. The minicolpostat configuration (8, 10) results in reduced shielding. Both the ovoid separation and the shields decrease the dose to the rectum and bladder (4, 6). When dealing with a narrow or anatomically distorted vaginal vault, the regular colpostats cannot be separated properly, and minicolpostats may have to be used, thereby increasing the bladder and rectal dose. This increases the risk for complications, since there is a correlation between complications and total dose to the bladder and rectum (12–15, 20). Knowledge of the geometric relationship between the organs at risk, namely, the bladder

Reprint requests to: Kenneth J. Weeks, Ph.D., Department of Radiation Oncology, Box 3295, Duke University Medical Center, Durham, NC 27710.

Acknowledgements—The authors gratefully thank Ron Overaker, Joe Owen, and Richard Nappi of the Duke University Instrument Shop for their skillful construction of the applicator. The authors also thank Jane Hoppenworth for her careful typing of text and figure illustrations for this manuscript. This work was supported in part by NCI Grant P30CA14236 and the Duke Comprehensive Cancer Center.

Accepted for publication 2 October 1996.

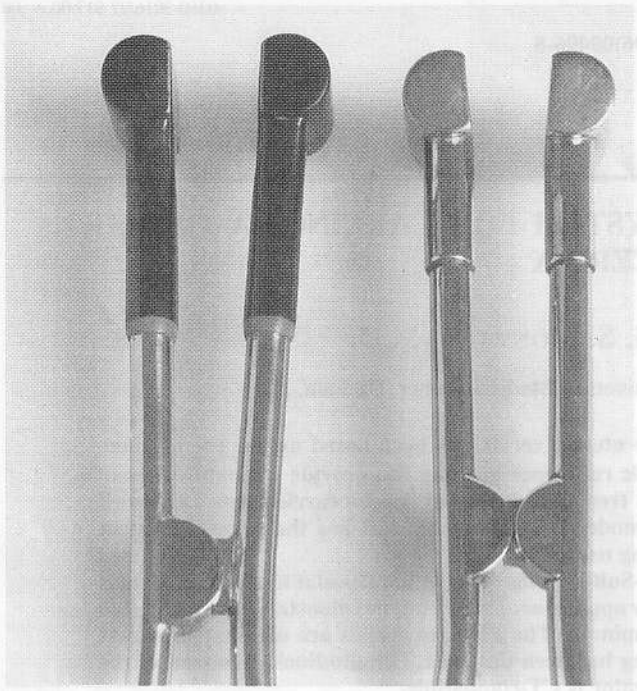

Fig. 1. Fletcher–Suit–Delclos colpostats (right) and the aluminum–steel colpostats (left) of the present work.

and rectum, and the shielded applicators is of paramount importance to determine the dose given to these organs (9). The traditional methods of calculating the dose to these organs with radiopaque contrast and markers is not sufficiently accurate. Previous investigators have noted (9, 11, 18) that computed tomography (CT) could be used to obtain a far more accurate characterization of the dose distribution. Toward the achievement of this goal, Weeks *et al.* (27) introduced a CT-compatible, modified plastic Fletcher applicator system. In that design, the Fletcher shields were attached to the source carrier and afterloaded into the applicator. Since the diameter of this shield is on the order of 12 mm, the colpostat handle diameter was enlarged (17, 27). The bulk of the applicator handles made placement in the patient more difficult, obscuring the view and hence precluding the routine use of this device. With further modification of this applicator (26), it is found to be satisfactory in about 50% of patients. The applicator devised in this work has none of those problems, since it is basically the same external shape as the Fletcher–Suit–Delclose (FSD). It is made possible by a new approach. The standard shields of the Fletcher applicator have been eliminated and shielding is achieved in a different manner, which will be described. This allows the applicator to be the same size as the standard Fletcher applicator, which is well known to work satisfactorily. The principal characteristics of this applicator are (a) full shielding effect with the minicolpostat configuration, (b) minimal interference with CT imaging, and (c) dose distribution and clinical use similar to the FSD.

METHODS AND MATERIALS

In this article, comparison is made to the stainless-steel FSD applicator (8). When the latter is used without any caps, it is referred to as a minicolpostat configuration and is denoted FSD-MC. In this configuration, the colpostat ovoid has a cross section in the shape of the letter *D*. The radius of curvature of the ovoid is 8 mm. Addition of a cap with shields produces a cylinder-like ovoid with diameter of 20 mm. Additional caps may be affixed to increase the diameter to 25 or 30 mm. A prototype of the new applicator has been constructed which has external dimensions and shape virtually identical to the FSD-MC. The tandems and ovoid heads are constructed from aluminum and are black-anodized. The colpostat handle and separation mechanism are made of stainless steel. Figure 1 shows the FSD-MC and the aluminum model described in this study. The ovoid internal structure is machined to produce a passageway (Fig. 2) to hold the source holder in position. The tandems (not shown) are replicas of the standard commercial shape, but are made of aluminum. The Fletcher-Suit (FS) shields are not used in this applicator. A new arrangement of tungsten metal was implemented. The source carrier is a singly machined piece of tungsten to which a steel inserter rod is attached with a steel pin. The tungsten carrier (Fig. 2) roughly resembles a half segment of a cylinder wall. The dimensions of the left colpostat tungsten source carrier are given in Table 1 in cylindrical coordinates for each of the sections W_1–W_6. Aluminum ovoid dimensions are also given in Table 1.

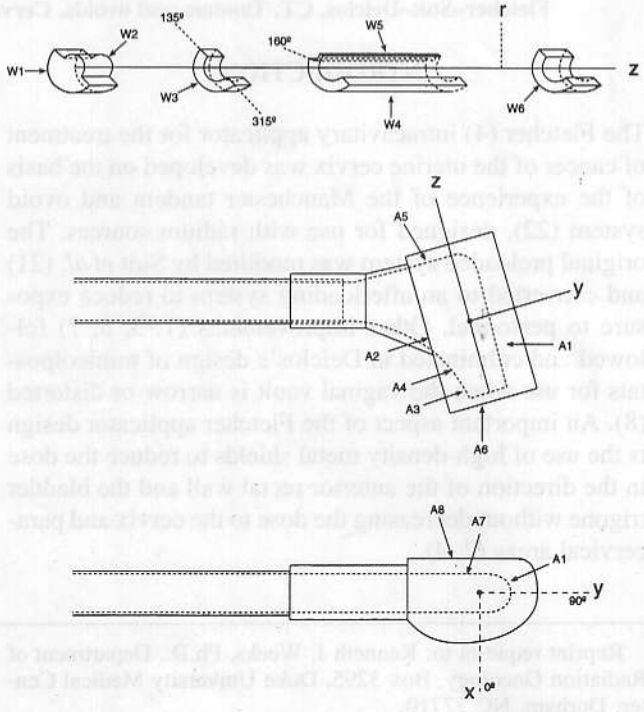

Fig. 2. (Upper) Exploded view of tungsten source carrier. (Middle) Side view of colpostat. (Lower) Top view of colpostat. Refer to Table 1 for dimensions.

Table 1. Coordinates (mm) for the computer modeling of the tungsten source carrier (W) and aluminum ovoid head (A)*

N	R_{min}	R_{max}	θ_{min}	θ_{max}	Z_{min}	Z_{max}
W_1	0	3	135	315	−13.5	−10.0
W_2	0	1.5	315	495	−13.5	−10.0
W_3	1.7	3.0	135	315	−10.0	−8.0
W_4	1.7	3.0	160	315	−8.0	6.3
W_5	1.7	2.1	135	160	−8.0	6.3
W_6	1.7	3.0	135	315	6.3	9.5
A_1	3.23	8.0	315	485	−13.5	12.5
A_2	7.0	8.0	235	315	−13.5	12.5
A_3	3.5	7.0	240	300	−13.5	−10.5
A_4	5.5	7.0	240	300	−10.5	−8.5
A_5†	0	8.0	0	360	12.5	14.5
A_6†	0	8.0	0	360	−14.5	−13.5
A_7†	3.23	7.0	125	235	−13.5	12.5
	X_{min}	X_{max}	Y_{min}	Y_{max}	Z_{min}	Z_{max}
A_8‡	−5.5	−4.0	−6.9	6.9	−14.5	14.5

* See Fig. 2 for coordinate system and general location.
† Piece is cut off by the plane $x = -4.0$ mm.
‡ Piece is a flat plate of aluminum which produces the flat part of the D shape.

The aluminum ovoid representation in A1–A8 approximately models the shape of the aluminum head. Cross-sectional views of the ovoid head are shown in the lower part of Fig. 2. The dimensions in Table 1 are those of the regular-shaped pieces which are used in the computer modeling to represent the smooth machine-finished product. The tungsten description (W_1–W_6) is almost exact. A thin steel clip (not shown in Fig. 2) is silver-soldered to the tungsten cylinder wall to keep the source centered on the bottom platform (W1 and W2 in Fig. 2). The radioactive source is dropped into the space between this clip and the tungsten wall (W_4).

The essence of the design of this applicator is that the cesium tube source is encapsulated in a semicylindrical filter of tungsten. Photons transversing the tungsten obliquely undergo greater attenuation than photons which are emitted perpendicular to the tungsten semicylinder. This is simply represented in Fig. 3. In the Fletcher applicators, the shields resemble sectors of a circular plate of given thickness. The sectors are placed in the applicators so that they will be between the cylindrical ^{137}Cs source and portions of the rectum and bladder. The radiation emitted in the direction of the protected tissue impinges on the shield in a direction approximately perpendicular. To increase the level of attenuation the thickness of the shield must be increased. To increase the area of tissue being protected, the radius must be increased. Note that in the Fletcher and FS (1, 4, 21) applicators, S_1 and S_2 (Fig. 3) are one piece and there is no minicolpostat configuration. The FSD design splits the traditional Fletcher upper and lower shield pieces into two pieces each (see S_1 and S_2 in Fig. 3a). The reason for this is that the flat side of the D must cut through the space occupied by the shield. One part of the upper and lower shields is built into the applicator (S_2 in Fig. 3a). The completing part (S_1 in Fig. 3a) of those two shields is incorporated into the plastic cylindrical caps which can be fit over the D-shaped ovoid head. In the minimal D-shaped ovoid head, no cap, and hence no shield S1 are present. Thus, an FSD application which uses the mini-ovoid (no caps) results in reduced attenuation relative to its FS-like configurations (caps on the FSD ovoids).

Referring to Fig. 3, the difference in relative attenuation effect between the present work and the FS design is schematically illustrated in two dimensions. Figure 3a illustrates the positioning of shielding S_1 and S_2 relative to the radiation source having a number of point sources a–f emitting radiation. It is clear that there is no differential attenuation from source elements a–f to tissue points T_1 and T_2. The strength of the radiation impinging on the rectum R is attenuated (shown in solid lines) by passage through attenuating material S_1 and S_2. A similar comparison could be made for the bladder B. In Fig. 3b, the present design accomplishes the reduction in dose to structure R by longitudinally aligning a material M_1 such that longer path lengths of material are traversed before radiation impinges upon R. In Fig. 3b, one notes that the material M_1 must be traversed in the path from the source to tissue point T_1. This produces a reduction in dose at T_1 relative to point T_2. However, this can be partially corrected by placing another material (M_2 in Fig. 3b) such that the dose to T_1 and T_2 is more closely balanced. Material M_1 in the present design is tungsten and is located in the source carrier. In fact, it is the source carrier. Material M_2 is aluminum and is located in the colpostat. In fact, it is piece A_1 in Table 1 and Fig. 2. This two-dimensional (2D) description is generalized to 3D using a computer. The radii, angles, and lengths were varied so that the final dose dis-

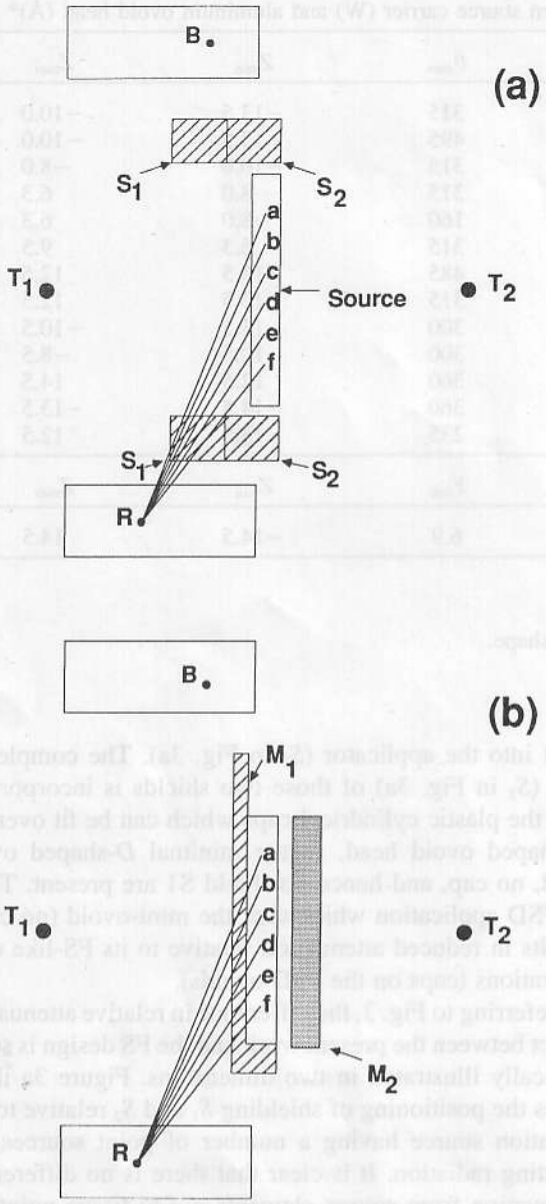

Fig. 3. (a) Schematic of traditional Fletcher ovoid shield concept. (b) Schematic of new ovoid shield concept. In both (a) and (b), T_1 is a point in tissue inferior to the ovoids, and T_2 is a tissue point superior, i.e., toward the cervix. R(B) signifies rectum (bladder).

tribution is similar to the FS. The final result is summarized in Table 1.

Dosimetric design of the new applicator was guided by the dose calculation and geometric algorithms presented previously (25). This algorithm was compared to experimental data, and once again, it was found (24, 25) that the inverse square effect and simple attenuation dominates the results. The effective attenuation coefficient (25) measured for aluminum is 0.016 cm^{-1} and the coefficient for tungsten is 0.123 cm^{-1}. The smallness of the aluminum attenuation coefficient shows that the aluminum has a mild effect on the dose rates. Measurements with a diode in a water phantom were used to confirm (24) the calculated results for the new applicator. The agreement (±3%) at close distances (<5 cm) was well within experimental measurement uncertainties and is adequate for clinical use. The asymmetric active source distribution of the commercial cesium source (19) was used in all the calculations, since that is the source which is used for the measurements. The dose rates calculated here for the 3M-FS agreed within a few percent of those presented by Williamson (28), despite the use of a different model for the cesium source. In the following, all dose-rate comparisons are normalized such that the dose rate from the various applicator designs is the same value at a distance of 3.0 cm from the radioactive source. If the source strength used for the 3M-FS ovoid is unity, then the source strength needed for the aluminum design is 1.014 and the source strength for the plastic design is 0.923. In other words, the aluminum ovoid attenuates the source 1.4% more than the 3M-FS, while the plastic applicator attenuates the source 8% less.

Results are presented below for both the aluminum prototype of this applicator and an obvious extension of this work to a plastic magnetic resonance imaging (MRI) compatible version. Schoeppel *et al.* (16) showed the ability of MRI to image tumor volume with the plastic applicators. Here, an aluminum prototype was produced instead of a plastic prototype because (a) it cost less, (b) MRI scans are not as readily accessible as CT ones, (c) no dummy source carriers (17, 26, 27) are needed, and (d) it allows real-time 3D CT-based dosimetry. The last two reasons arise because the aluminum construction of the tandem and ovoids makes identification of the applicator components in each CT image slice relatively easy. As can be seen in Fig. 4, both the tandem and ovoids are clearly visualized. This obviously makes the applicator capable of being very quickly delineated in the CT scan data using thresholding techniques. The 3D treatment planning (23) can thus be automated and can be performed

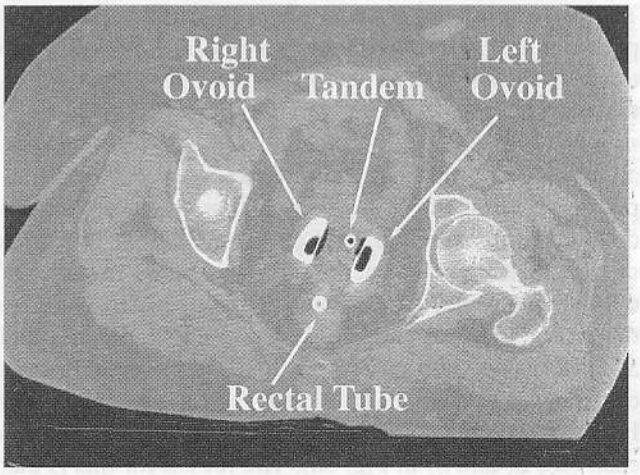

Fig. 4. Computed tomography scan image showing tandem, rectal tube, and left and right ovoid cross sections.

in a short period of time, allowing the CT-based treatment planning to be completed before the applicator needs to be loaded.

RESULTS

We begin by considering the dose differences for a single ovoid. Figure 5 shows a cross section of the left colpostat's ovoid along with a Cartesian coordinate system and reference points for dose-rate comparison. Table 2 contains a comparison of calculated dose rates at these points. The point $x = 0$, $y = 0$, $z = 0$ is centered in the ovoid. The y-axis is perpendicular to the plane of the figure. As is well known, plastic caps are used to increase ovoid diameter whenever patient anatomy can accommodate them. The bare (no cap) configuration of the ovoid is denoted "mini". A 20-mm (outer diameter) plastic cylindrical shell can be placed over the D and thereby form the small configuration. Similarly, a 25-mm (30-mm) plastic cap produces medium (large) configurations. For any design, the larger the cap is, the lower is the ovoid surface dose rate. The caps increase the radius (R) and width (W) of the ovoid. R and W are defined in Fig. 5 and their values are given in Table 2. The Aluminum D cap is a completely separate new configuration. In Table 2, points P_1 and P_2 were used to set the normalization of the strengths of the sources; thus, the dose at these points are identical for all configurations. The dose at the vaginal surface is represented by the calculations at S_1, S_2, and S_3. Comparing the mini configurations, the dose at S_3 for the Al-mini or the plastic mini is less than the 3M-FSD value, even though the dose rates at S_1 and S_2 are no different. This is because the new mini design has a slightly larger width but the same radius of curvature.

An advantage of the new design is that regardless of cap configuration, the rectum and bladder are shielded to the same extent. This is seen by comparing the results for the Al-mini to the Al-small and medium for the R and B points in Table 2. Comparison of the Al mini to the 3M-mini results for the R and B plane points in Table 2 shows that the dose rates are less for the Al-mini except for points R_3, B_1, and B_6. Overall, the dose is less to the regions above and below the ovoids with the new design of shield. The results for the plastic mini version of the new design are also given in Table 2. Almost all differences of point dose rates are a little larger when comparing plastic (instead of aluminum) to the 3M design. Once the 3M-FSD small caps are put on, the 3M-small shields the points above and below the ovoid quite a bit better than the 3M-mini (see points R_7, R_8, and R_{10}). The 3M-small and the Al-small are a closer comparison than for the minis because the 3M-small is now fully shielded. Since even for the 3M design, going to the medium configuration is just adding more plastic; the medium results are basically unchanged from the small, except for a reduction in ovoid surface dose rates. The new aluminum D-cap results are noteworthy. The dimensions for the D-cap in Table 2 result in a smaller ovoid volume than the small configuration. However, the surface dose rates for S_1 and S_2 are the same as the 20-mm (small) cap results. Furthermore, the rectal and bladder planes are fully shielded, but the width is close to 3 mm less. Hence, this intermediate minicolpostat cap may obviate some of the objections to using minicolpostats (namely, vaginal mucosa complications).

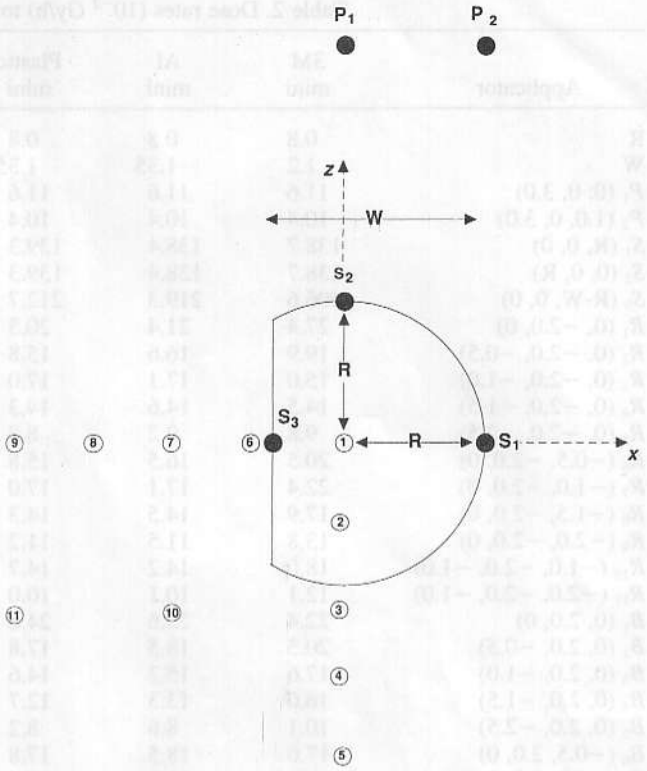

Fig. 5. Left ovoid cross section for defining points for Table 2 dose-rate comparison. The y axis is perpendicular to page. Points P_1, P_2, S_1, S_2, and S_3 lie in the plane of the figure ($y = 0$). Points B_1–B_{11} and R_1–R_{11} lie at the locations of labels 1 . . . 11, but are 2.0 cm above and below the plane of the figure, respectively. The width (W) of the ovoid and the radius of curvature (R) are defined.

Figure 6 shows a comparison between dose rates calculated for a FS and the new aluminum ovoid. Figure 6a shows the comparison in a coronal plane which is 1.0 cm below the bottom of the ovoid ($z = -25$ mm). In the upper right quadrant ($x > 0$, $y > 0$), the results are virtually identical. One sees that in the shielded regions ($x < 0$, $y \leq 0$), the protection difference afforded by the two designs is variable. The 0.12 Gy/h line is pulled farther in (toward the origin) for the aluminum design, whereas the 0.10 Gy/h line is farther in for the FS. The presence of the 0.10 Gy/h island region for the aluminum distribution indicates that the dose rate for the aluminum is fairly constant between the island 0.10 Gy/h isodose line and the outer 0.10 Gy/h line. Farther to the patient's right ($x < -1.5$ cm), the longitudinal tungsten design causes all of the aluminum dose rates to be less than the FS. The middle part of

Table 2. Dose rates (10^{-2} Gy/h) to labeled points [x, y, z (in cm)] in Fig. 5

Applicator	3M mini	Al mini	Plastic mini	Al *D* cap	3M small	Al small	3M medium	Al medium
R	0.8	0.8	0.8	1.0	1.0	1.0	1.25	1.25
W	1.2	1.35	1.35	1.73	2.0	2.0	2.5	2.5
P_1 (0, 0, 3.0)	11.6	11.6	11.6	11.6	11.6	11.6	11.6	11.6
P_2 (1.0, 0, 3.0)	10.4	10.4	10.4	10.4	10.4	10.4	10.4	10.4
S_1 (R, 0, 0)	138.7	138.4	139.3	94.1	94.3	94.1	63.0	62.9
S_2 (0, 0, R)	138.7	138.4	139.3	94.1	94.3	94.1	63.0	62.9
S_3 (R-W, 0, 0)	406.6	219.3	212.7	192.2	94.9	82.7	63.4	55.4
R_1 (0, −2.0, 0)	27.4	21.4	20.3	21.4	27.4	21.4	27.4	21.4
R_2 (0, −2.0, −0.5)	19.9	16.6	15.8	16.6	19.9	16.6	19.9	16.6
R_3 (0, −2.0, −1.0)	15.0	17.1	17.0	17.1	15.0	17.1	15.0	17.1
R_4 (0, −2.0, −1.5)	14.5	14.6	14.3	14.6	14.5	14.6	14.5	14.6
R_5 (0, −2.0, −2.5)	9.8	9.2	8.8	9.2	9.8	9.2	9.8	9.2
R_6 (−0.5, −2.0, 0)	20.5	16.5	15.8	16.5	20.5	16.5	20.5	16.5
R_7 (−1.0, −2.0, 0)	22.4	17.1	17.0	17.1	15.8	17.1	15.8	17.1
R_8 (−1.5, −2.0, 0)	17.9	14.5	14.3	14.5	15.0	14.5	15.0	14.5
R_9 (−2.0, −2.0, 0)	13.8	11.5	11.2	11.5	13.1	11.5	13.1	11.5
R_{10} (−1.0, −2.0, −1.0)	18.0	14.2	14.7	14.2	15.2	14.2	15.2	14.2
R_{11} (−2.0, −2.0, −1.0)	12.1	10.1	10.0	10.1	11.8	10.1	11.8	10.1
B_1 (0, 2.0, 0)	22.4	25.6	24.6	25.6	22.4	25.6	22.4	25.6
B_2 (0, 2.0, −0.5)	20.3	18.5	17.8	18.5	20.3	18.5	20.3	18.5
B_3 (0, 2.0, −1.0)	17.6	15.2	14.6	15.2	17.6	15.2	17.6	15.2
B_4 (0, 2.0, −1.5)	16.0	13.3	12.7	13.3	16.0	13.3	16.0	13.3
B_5 (0, 2.0, −2.5)	10.1	8.6	8.2	8.6	10.1	8.6	10.1	8.6
B_6 (−0.5, 2.0, 0)	17.0	18.5	17.8	18.5	17.0	18.5	17.0	18.5
B_7 (−1.0, 2.0, 0)	19.4	14.5	14.6	14.5	13.2	14.5	13.2	14.5
B_8 (−1.5, 2.0, 0)	16.0	12.8	12.6	12.8	14.3	12.8	14.3	12.8
B_9 (−2.0, 2.0, 0)	12.6	10.5	10.2	10.5	12.5	10.5	12.5	10.5
B_{10} (−1.0, 2.0, −1.0)	16.8	12.4	13.0	12.4	14.5	12.4	14.5	12.4
B_{11} (−2.0, 2.0, −1.0)	11.2	9.3	9.2	9.3	11.2	9.3	11.2	9.3

Fig. 6 (a coronal plane which bisects the ovoid) clearly shows the complete agreement throughout the upper diagonal portion of this plane. It also shows the relative reduction of dose behind the ovoid. In the lower part of Fig. 6 (1.0 cm above the ovoid) the difference in dose is similar to Fig. 6a except that the new design's shielding is not cut off in the region $x > 0$, $y < 0$, as is traditionally done in the FS [namely, 150° upper bladder shield (4) as opposed to 180° lower-rectum shield]. Thus, the isodose lines are contracted in that region.

If the aluminum applicator body is replaced by plastic, the material M_2 of Fig. 3 produces negligible attenuation. Plastic M_2 thus cannot help balance out the radial attenuation of piece M_1. Thus, additional differences between the FSD and the plastic applicator dose distributions arise. Figure 7 shows a dose-rate comparison for aluminum and plastic construction of the ovoid, respectively. Figure 7b shows complete agreement in the upper right diagonal region. There are small discrepancies in the upper (z = 2.5-cm) and lower (z = −2.5-cm) planes. Figure 7 does indicate that the differences between the aluminum and plastic designs of the new applicator are clinically insignificant.

One is primarily interested in the total dose distribution arising from the tandem and ovoids together. Figure 8 shows a direct comparison between the total dose-rate distributions for the FS and the aluminum model with five sources loaded into each applicator. The strengths of the sources in the tandem were 108, 72, 72 μGy m^2/h in the tandem and 108 μGy m^2/h in each of the ovoids (corresponding to a 15–10–10 15–15 mg Ra eq. historical standard loading). A CT coordinate system is used with the z axis running from foot to head. For simplicity, the ovoids are centered exactly at $y = 0$, $z = 0$, and $x = \pm 2.0$ cm, and a perfectly straight tandem exactly bisects the ovoids. The three cesium sources in the tandem are centered at $x = 0$, $y = 0$, and z = 5.0, 3.0, and 1.0 cm, respectively. The upper left of Fig. 8 shows a sagittal dose-distribution comparison. The aluminum (solid line) result is reduced inferior to the ovoids ($z < 0$). The upper right of Fig. 8 shows an axial ($z = 0$) plane bisecting the two ovoids. Laterally from the ovoids ($|x| > 3.0$ cm) the differences are negligible. Between the ovoids (for $|y| < 1.0$ cm), the differences are not significant. Anterior and posterior dose rate differences are seen between the ovoids ($|x| <$ 2.0 cm, $|y| > 1.0$ cm); for the most part, the dose rate is less with the new design. The lower left of Fig. 8 shows a coronal plane which is centered in the applicator and which passes through all the sources in both tandem and ovoids. Again, the new design has reduced dose behind ($z < 0$) the ovoids. The lower right of Fig. 8 gives the results in a coronal view 1.0 cm below the bottom of the ovoids

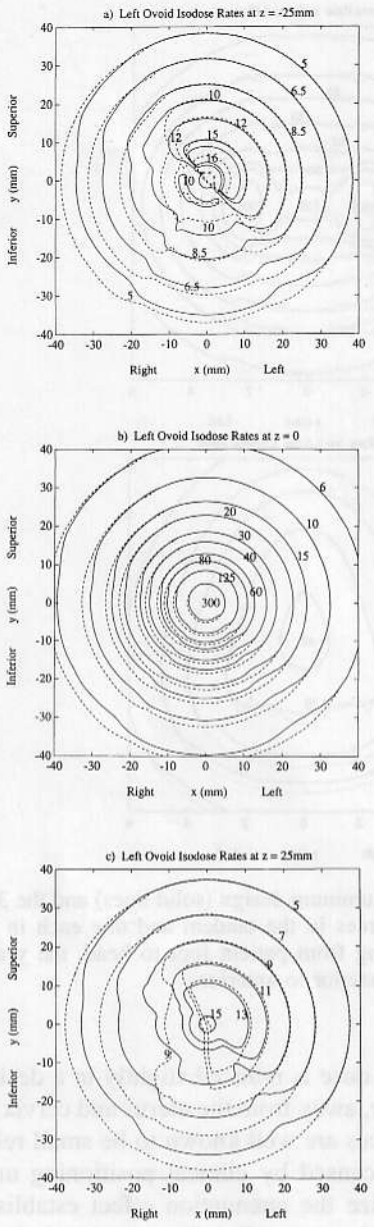

Fig. 6. Left ovoid shielded dose rate (10^{-2} Gy/h) coronal plane comparisons for a 108-μGy m^2/h cesium source in the 3M-FS (dashed line) and a 109.6-μGy m^2/h cesium source in the aluminum ovoid (solid lines).

($y = -2.5$ cm). The differences are confined to the region behind the ovoids.

DISCUSSION

A very significant portion of the total dose required to treat carcinoma of the cervix definitively with radiation therapy is administered by brachytherapy. With brachytherapy, a high dose of radiation is given to the cervix, paracervical tissues, and normal structures in the vicinity of the cervix and parametria, namely, the bladder and rectum. The probability of achieving local control of the tumor in the cervix and paracervical areas and the development of complications are dose dependent. The portion of the dose of radiation given with the intracavitary therapy can be very significant. It is therefore important to calculate this dose accurately, as the positioning of the applicator in relationship to the tumor in the cervix as well as the surrounding normal structures is variable from patient to patient. The dose has been calculated historically from orthogonal films. It has been recognized (9) that a true 3D analysis of this therapy is a reasonable goal. This can only be accomplished using CT or MRI imaging modalities to determine the spatial relationship of the critical structures and the applicator.

The CT applicators designed previously (26, 27) permitted the use of CT dosimetry and allowed for the use

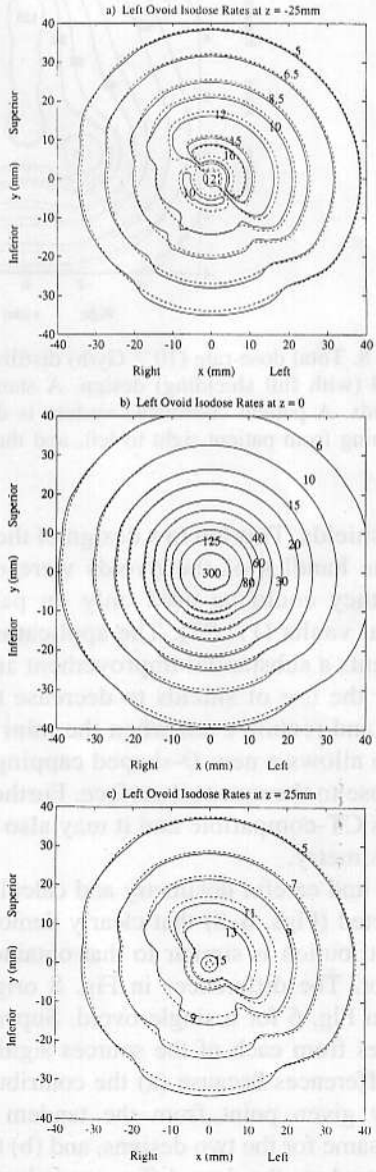

Fig. 7. Left ovoid dose rate (10^{-2} Gy/h) coronal plane comparisons for a 102-μGy m^2/h cesium source in a plastic ovoid (dashed line) and a 109.6-μGy m^2/h cesium source in an aluminum ovoid (solid line), both of the new design.

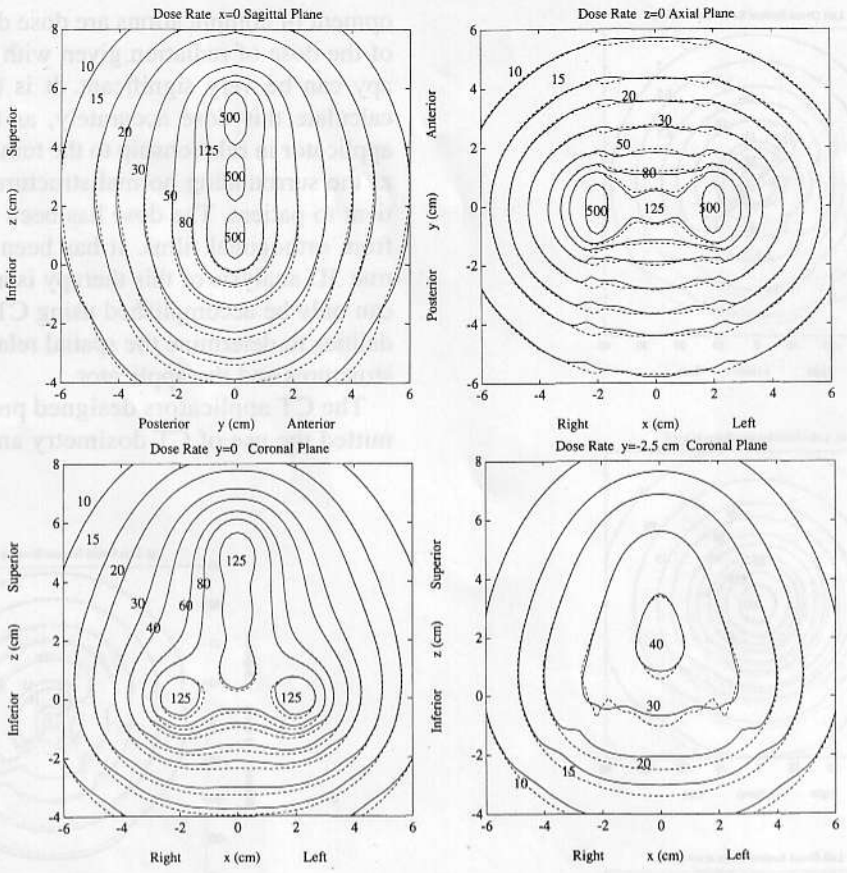

Fig. 8. Total dose-rate (10^{-2} Gy/h) distribution comparison between the aluminum design (solid lines) and the 3M-FSD (with full shielding) design. A standard loading is used: three sources in the tandem and one each in the ovoids. A patient coordinate system is defined here as the z axis running from patient foot to head, the y axis running from patient right to left, and the y axis running from patient posterior to anterior.

of Fletcher shields. This led to a design of the applicator in which the handles of the ovoids were quite wide. Therefore, they could be used only on patients with large vaginal vaults (17, 27). The applicator described here represents a substantial improvement and makes it possible for the use of shields to decrease the dose to the bladder and rectum even when the mini ovoids are used. It also allows a new *D*-shaped capping which reduces the dose to the mucosal surface. Furthermore, the applicator is CT-compatible and it may also be adapted for MRI dosimetry.

Extensive and careful dosimetry and calculations have been conducted (Figs. 6–8) that clearly demonstrate that the dose distribution is similar to that obtained with the FS applicator. The differences in Fig. 8 originate from those seen in Fig. 6 for a single ovoid. Superposition of the dose rates from each of the sources significantly reduces the differences because (a) the contribution of the dose to any given point from the tandem sources is roughly the same for the two designs, and (b) the position in the patient where the dose difference is largest for one ovoid is not the same position for the other ovoid. The main differences lie inferior ($z < 0$) to the ovoids. The differences do not seem to be unfavorable for the new design. The dose is reduced slightly in a desirable direction (namely, away from the uterus and cervix). However, the differences are well known to be small relative to the differences caused by clinical positioning uncertainties. To summarize the attenuation effect established by the present work, generally the same relative result is achieved as in the FS for the critical organs and tumor-bearing structures such as cervix, vaginal fornices, and uterus. However, a different pattern is created inferior to the ovoids. In short, a new 3D dose distribution is created which is equivalent in the crucial regions and different in the other regions (the main difference is that the dose is less).

This applicator is now being used routinely and no problems have been encountered. With respect to the dosimetry characteristics of this applicator relative to the standard FS applicator and other applicators available, at this point the reduced dose behind the ovoids is simply a theoretical consideration, since it would take a long time to demonstrate any clinical difference. Given the many other variables that determine the outcome on the treatment of patients with carcinoma of the cervix with radiation therapy, it would not be possible to test the dosimetric differences of this applicator in a meaningful

way clinically. On the other hand, the data being collected now with this applicator with respect to the 3D dosimetry can certainly be compared with the film-based 3D dosimetry data available. This provides an ongoing method of evaluation that will also allow for refinements of this applicator and development of more accurate and reliable methods of dose prescription for carcinoma of the cervix, which has been a recommendation of the International Commission on Radiation Units and Measurements report (9). It will also allow retrospective evaluation of complications with 3D dose distributions contributing to the knowledge of normal tissue tolerances in radiation therapy. This work will be presented in the future.

REFERENCES

1. Delclos, L.; Fletcher, G. H.; Moore, E. B.; Sampiere, V. A. Minicolpostats, dome cylinders, other additions and improvements of the Fletcher-Suit afterloading system: Indications and limitations of their use. Int. J. Radiat. Oncol. Biol. Phys. 6:1195–1206; 1980.
2. Delclos, L.; Fletcher, G. H.; Sampiere, V.; Grant, W. H. Can the Fletcher gamma ray colpostat system be extrapolated to other systems? Cancer 41:970–979; 1978.
3. Delclos, L; Fletcher, G. H.; Suit, H. D.; Sampiere, V.; Moore, B. Afterloading vaginal irradiators. Radiology 96:666–667; 1970.
4. Fletcher, G. H. Cervical radium applicators with screening in the direction of bladder and rectum. Radiology 60:77–84; 1953.
5. Green, A. E.; Broadwater, J. R.; Hancock, J. A. Afterloading vaginal ovoids. AJR 105:609–613; 1969.
6. Haas, J. S.; Dean, R. D.; Mansfield, C. M. Dosimetric comparison of the Fletcher family of gynecologic colpostats 1950–1980. Int. J. Radiat. Oncol. Biol. Phys. 11:1317–1321; 1985.
7. Haas, J. S.; Dean, R. D.; Mansfield, C. M. Evaluation of a new Fletcher applicator using Cesium-137. Int. J. Radiat. Oncol. Biol. Phys. 6:1589–1595; 1980.
8. Haas, J. S.; Dean, R. D.; Mansfield, C. M. Fletcher-Suit-Delclos gynecologic applicator: Evaluation of a new instrument. Int. J. Radiat. Oncol. Biol. Phys. 9:763–768; 1983.
9. ICRU Report 38: Dose and volume specification for reporting intracavitary therapy in oncology. Bethesda, Maryland: International Commission on Radiation Units and Measurements; March 1, 1985.
10. Kuske, R. R.; Perez, C. A.; Jacobs, A. J.; Slessinger, E. D.; Hederman, M. A.; Walz, B. J.; Kao, M. S.; Camel, H. M. Mini-colpostats in the treatment of carcinoma of the uterine cervix. Int. J. Radiat. Oncol. Biol. Phys. 14:899–906; 1988.
11. Ling, C. C.; Schell, M. C.; Working, K. R.; Jentzsch, K.; Harisiadis, L.; Carbell, S.; Rogers, C. C. CT-assisted assessment of bladder and rectum dose in gynecological implants. Int. J. Radiat. Oncol. Biol. Phys. 13:1577–1582; 1987.
12. Montana, G. S.; Fowler, W. C. Carcinoma of the cervix: Analysis of bladder and rectal radiation dose and complications. Int. J. Radiat. Oncol. Biol. Phys. 16:95–100; 1989.
13. Montana, G. S.; Fowler, W. C.; Varia, M. A.; Walton, L. A.; Mack, Y.; Shemanski, L. Carcinoma of the cervix, Stage III. Results of radiation therapy. Cancer 57:148–154; 1986.
14. Perez, C. A.; Breaux, S.; Bedwinek, J. M.; Madoc-Jones, H.; Camel, H. M.; Purdy, J. A.; Walz, B. J. Radiation therapy alone in the treatment of carcinoma of the uterine cervix. Cancer 54:235–246; 1984.
15. Porquier, H.; Dubois, J. B.; Delard, R. Cancer of the uterine cervix: Dosimetric guidelines for prevention of late rectal and rectosigmoid complications as a result of radiotherapeutic treatment. Int. J. Radiat. Oncol. Biol. Phys. 8:1887–1895; 1982.
16. Schoeppel, S. L.; Ellis, J. H.; LaVigne, M. L.; Schea, R. A.; Roberts, J. A. Magnetic resonance imaging during intracavitary gynecologic brachytherapy. Int. J. Radiat. Oncol. Biol. Phys. 23:175–181; 1992.
17. Schoeppel, S. S; Fraass, B. A.; Hopkins, M.; LaVigne, M. L.; Lichter, A. S.; McShan, D. L.; Noffsinger, S.; Perez-Tamayo, C.; Roberts, J. A. A CT-compatible version of the Fletcher system intracavitary applicator: Clinical application and 3-dimensional treatment planning. Int. J. Radiat. Oncol. Biol. Phys. 17:1103–1109; 1989.
18. Sewchand, W.; Prempree, T.; Patanaphan, V.; Whiteley, N. O.; Heidtman, B.; Scott, R. M. Value of multi-planar CT images in interactive dosimetry planning of intracavitary therapy. Int. J. Radiat. Oncol. Biol. Phys. 8:295–301; 1982.
19. Sharma, S. C.; Williamson, J. F.; Khan, F. M.; Jones, T. K. Dosimetric consequences of asymmetric positioning of active source in 137-Cs and 226-Ra intracavitary tubes. Int. J. Radiat. Biol. Phys. 7:555–559; 1981.
20. Strockbine, M. F.; Hancock, J. E.; Fletcher, G. H. Complications in 831 patients with squamous cell carcinoma of the intact uterine cervix treated with 3000 Rads or more whole pelvis irradiation. AJR Radium Ther. Nucl. Med. 108:293–304; 1970.
21. Suit, H. D.; Moore, E. B.; Fletcher, G. H.; Worsnop, M. A. Modification of Fletcher ovoid system for afterloading, using standard-sized radium tubes (milligram and microgram). Radiology 81:126–131; 1963.
22. Tod, M. C.; Meredith, W. J. Dosage system for cancer of the cervix. Br. J. Radiol. 11:809–823; 1938.
23. Weeks, K. J. Brachytherapy visualization using AVS. In 1994 International AVS Users Group Conference Proceedings. Boston, MA; 1994:437–443.
24. Weeks, K. J.; Das, S.; Price, E. Measured dose distributions for a new CT compatible tandem and ovoids system. Med. Phys. 21:899; 1994.
25. Weeks, K. J.; Dennett, J. C. Dose calculation and measurements for a CT compatible version of the Fletcher applicator. Int. J. Radiat. Oncol. Biol. Phys. 18:1191–1198; 1990.
26. Weeks, K. J.; Montana, G. S.; Bentel, G. C. Design of a plastic minicolpostat applicator with shields. Int. J. Radiat. Oncol. Biol. Phys. 21:1045–1052; 1991.
27. Weeks, K. J.; Schoeppel, S. S; Pruss, K.; Hopkins, M.; Perez-Tamayo, C. A computed tomography compatible afterloading Fletcher-Suit-Delclos colpostat with adjustable shielding. Endocuriether. Hypertherm. Oncol. 5:169–174; 1989.
28. Williamson, J. F. Dose calculations about shielded gynecological colpostats. Int. J. Radiat. Oncol. Biol. Phys. 19:167–178; 1990.